

Selective Two-photon Excitation by Parametrically Shaped Laser Pulses after an Optical Fiber

Albrecht Lindinger

Institut für Experimentalphysik, Freie Universität Berlin, Arnimallee 14, D-14195 Berlin, Germany

Keywords: Pulse Shaping, Optical Fibers, Multi-photon Processes.

Abstract: Laser pulse shaping through optical fibers is reported for applications on two-photon processes in dye molecules. The presented method utilizes pre-compensation of the optical fiber properties by analytical pulse shaping in order to receive specific parametric pulse forms after the fiber including polarization modulation. Particularly phase-tailored pulse shapes at the distal fiber end are employed for two-photon fluorescence of dyes in a liquid environment in order to improve the contrast between dye markers having similar excitation spectra. This will lead to new endoscopic imaging applications with an increased fluorescence contrast.

1 INTRODUCTION

Coherent control of photo-induced molecular processes by shaped laser pulses has attained considerable success in recent years. It became most exciting when self-learning feedback loop algorithms were employed where tailored laser pulses can be generated, which drive the induced processes at a maximum yield along desired paths (Judson and Rabitz, 1992); (Brixner and Gerber, 2003). An important issue in this regard is the information coded in the optimized laser pulse shape which supplies insight about the underlying processes (Schäfer-Bung et al., 2004).

In the last years polarization pulse shaping was explored in order to consider the vectorial character of the light field (Brixner and Gerber, 2001); (Polachek et al., 2006). Novel pulse shaper schemes for simultaneous phase, amplitude, and polarization pulse control were designed, and a parametric sub pulse encoding was developed (Weise and Lindinger, 2010). In this approach, the physically intuitive parameters energies, distances, and chirps, as well as the states of polarization of the sub pulses can be controlled. This yields new perspectives of adding the polarization and hence utilizing all properties of the light field in the pulse modulation.

Recently, pulse shaping methods were increasingly used in life sciences in order to investigate biologically relevant systems (Herek et

al., 2002). Promising applications are imaging using multi-photon microscopy, spectroscopy, and photodynamic therapy (Myaing et al., 2006); (König, 2000); (Tsen et al., 2007). Laser pulse shaping was moreover applied to multi-photon excited fluorescence where interference effects are utilized (Meshulach and Silberberg, 1998). This enables to achieve narrow band transitions and can be used to selectively excite different biologically relevant fluorophores with close lying excitation bands (Lozovoy et al., 2002); (Ogilvie et al., 2006).

In order to operate in biologically relevant environments, in vivo applications are desired where the light is guided to the place of interest. This can be realized by transmission of light through optical fibers for endoscopic applications, which is a novel topic of large relevance e.g. for medical treatments. Yet, it is challenging to transfer femtosecond laser pulses through fibers due to the occurring distortion of the intense light pulses by linear and nonlinear optical fiber properties (Agrawal, 2001). Successful guidance of ultrashort laser pulses would however enable novel endoscopic imaging and therapeutic feasibilities.

In this contribution, laser pulse shaping will be combined with optical fibers and biologically relevant multi photon spectroscopy. Tailored laser pulses are guided through hollow core photonic crystal fibers, and predetermined parametrically shaped laser pulses in phase, amplitude and polarization are achieved after the fiber by

considering the linear, nonlinear, and polarization fiber properties. This enables to steer photoinduced processes by utilizing these pulses for multi-photon excitation in molecular systems. The application of phase-tailored pulses for imaging contrast enhancement is finally demonstrated for dye molecules in a liquid after transmitting a hollow core photonic crystal fiber.

2 EXPERIMENT

The experimental setup consists of a femtosecond laser system (Mira oscillator, RegA amplifier, Coherent Inc.) which delivers 60 fs pulses at 805 nm central wavelength with a repetition rate of 76 MHz for the oscillator and 286 kHz for the amplifier. Pulse shaping is performed by a spatial light modulator (SLM640, CRi) placed in the Fourier plane of a 4f-setup for the dye experiments and combined with another modulator (SLM256, CRi) and a polarizer in between for the polarization modulated pulses. The center pixels of the pulse modulator are aligned to the central wavelength of 805 nm. A wave plate is placed in the beam after the pulse shaper in order to align the light polarization parallel to the optical axes of the fiber. The pulses are subsequently coupled into a hollow core photonic crystal fiber (HC-800-1, NKT Photonics). The core of this fiber measures 9.2 μm for the short axis and 9.5 μm for the long axis. The transmission window is centered at 830 nm and about 70 nm wide. The zero dispersion wavelength is located at 805 nm and the third order Taylor term of the dispersion function dominates for these pulses. Laser pulses utilized in this contribution exhibit negligible non-linear effects in the fiber. A telescope is used to modify the beam diameter for adequate coupling into the fiber. After the fiber, the laser beam is widened by a telescope for the dye experiment and focused into a cuvette containing rhodamine B ($2.5 \cdot 10^{-4}$ molar) and coumarin 1 ($7.5 \cdot 10^{-3}$ molar) solved in ethanol.

Since the exact spectral phase of the laser pulses at the cuvette is crucial for the measurements, its distortion by the optical elements is compensated by writing the corresponding phase retardances on the pulse modulator. The fluorescence light is collected by two lenses and then detected by a fiber spectrometer. The fluorescence of the two dyes is spectrally well separated, which enables to record the excitation efficiency by integrating from 410 nm to 550 nm for coumarin 1 and 560 nm to 700 nm for rhodamine B.

The shaped pulses are detected after the fiber by using a time resolved ellipsometry scheme. It is based on a sum frequency generation cross correlation setup using a BBO crystal (Plewicki et al., 2006). The shaped pulse is convoluted with a short reference pulse received directly from the laser. The BBO crystal is polarization sensitive and selects only the intensity in one polarization direction. A set of cross correlation traces is recorded by rotating the polarization of the shaped pulse using a half-wave plate. For each time step the instantaneous ellipse of the electrical field can be determined. This data is presented in a single graph in which the time-dependent intensity and polarization state including ellipticity and orientation are displayed. The ellipticity is defined as the ratio of the major to minor axis. A three-dimensional representation of the pulse is calculated based on the measured data.

3 PULSE SHAPING THROUGH FIBERS

Ultrashort laser pulses guided through optical fibers are affected by the intrinsic optical fiber properties which have influence on the spectral distribution and the temporal evolution of the transmitted pulses. Particularly the dispersion, birefringence and nonlinearity of the fiber have to be considered. These properties can be determined by utilizing the pulse shaper. Generally, spatial light modulator phase values are searched for in order to pre-compensate the laser pulse such that one receives a short pulse after the fiber.

Novel hollow core photonic crystal fibers are utilized here since they are advantageous for guiding ultrashort pulses due to the light propagation in the hollow core and hence their minor dispersion and nonlinearity (Russel, 2003). The asymmetric shape of the hollow fiber core leads to large birefringence. This causes a temporal separation of the components after propagation through the fiber with each component chirped differently. Therefore, the fiber can be described by two perpendicular optical axes, which have different dispersions. These axes are denoted as fast (f) and slow (s) axes due to the different group velocities. If light is linearly polarized along one of these axes, the state of polarization is not altered by the fiber. The overall orientation of the polarization shaped pulse is determined by the orientation of the optical axis of the fiber. Both sub pulses are still linearly polarized

and oriented along the respective optical axes after propagation through the fiber. The temporal intensity profiles are asymmetric and broadened due to chromatic dispersion of the fiber. This broadening and asymmetry, which is characteristic for second and third order phase functions, can be compensated for by applying a phase function of the opposite sign on each pulse in order to produce short sub pulses after the fiber. These values corresponding to the respective axes are written as an offset on the modulator. The delay between the differently polarized pulse components is attributed to the difference in the group velocity and can as well be pre-compensated with the pulse shaper. Finally, the relative phase between the two pulses is adjusted to generate a single linearly polarized output pulse oriented at 45° . Having this compensation determined, the pulse which is transmitted through the fiber can be arbitrarily controlled in phase, amplitude, and polarization.

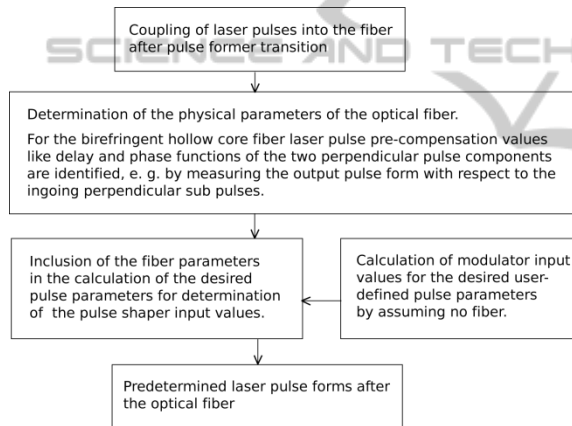


Figure 1: Block diagram of the parametric pulse shaping method through optical fibers.

For the birefringent hollow core fiber the orientation of the output pulse can be changed by altering the relative amplitudes of the two polarization components. The shift of the relative phase between the components results in a change of the ellipticity (Weise et al., 2010). This procedure can be extended to pulse sequences consisting of a variable number of sub-pulses. Any individual sub-pulse is generated by two perpendicularly polarized pulses whose energy ratio, relative phase, and delay are set. Parametric sub-pulse sequences for each polarization component are produced by following the method described in ref. (Weber et al., 2005). Minor side pulses still occur for the employed pulse shaper setup, yet they can be removed by a more

advanced pulse shaper design (Weise and Lindinger, 2010).

The determined fiber precompensation phase functions and the fiber phase difference are included in the calculation of the phase retardances of the liquid crystal arrays by adding the corresponding phase values. The required electric fields at the proximal end of the fiber can be generated with the appropriate phase retardances of the liquid crystal arrays. Hence, combining the desired sub-pulse sequence phase values with the pre-compensation phase parameters controls the shape of the laser pulse after the fiber (see Figure 1 for a comprehensive method description).

Parametric control of sub-pulses in a pulse sequence delivered by the Mira oscillator is illustrated for a series of double pulses, where one parameter of the pulse sequence is independently controlled (Figure 2). The double pulses are constructed from three sub pulse components. The first sub-pulse in these pulse sequences is linearly polarized parallel to the slow axis of the fiber. The two other sub pulse components yield the second sub-pulse. The experimental application of a linear chirp on the second sub-pulse and the associated increase in pulse duration is presented in Figure 2(a). The rotation of a sub-pulse is demonstrated in Figure 2(b). Both sub-pulses are linearly polarized while the orientation of the second sub-pulse is changed from 0 to 150° . The control of the ellipticity from linear to circular is visualized in Figure 2(c) in which the second sub-pulse is oriented at -45° relative to the slow axis of the fiber. These data prove the good agreement of the set parameters with the measured parameters of the shaped pulses.

This procedure is not limited to double pulses and can be extended to a larger number of sub-pulses and higher complexity, which is exemplified in Figure 3 where a triple pulse sequence is depicted with differently chirped and polarized sub-pulses.

The example shows the potential of laser pulse shaping after optical fibers which can be employed for various optical applications. Even nonlinear fiber properties leading dominantly to self-phase modulation can be controlled by pre-calculating the input laser pulse shape with back-propagating the nonlinear Schrödinger equation (Tsang et al., 2003); (Pawłowska et al., 2012). In the following, pulse shaping via fibers applied to two-photon dyes will be demonstrated for one polarization direction in the linear regime, but it can in principle be extended to differing polarization directions and to the nonlinear regime.

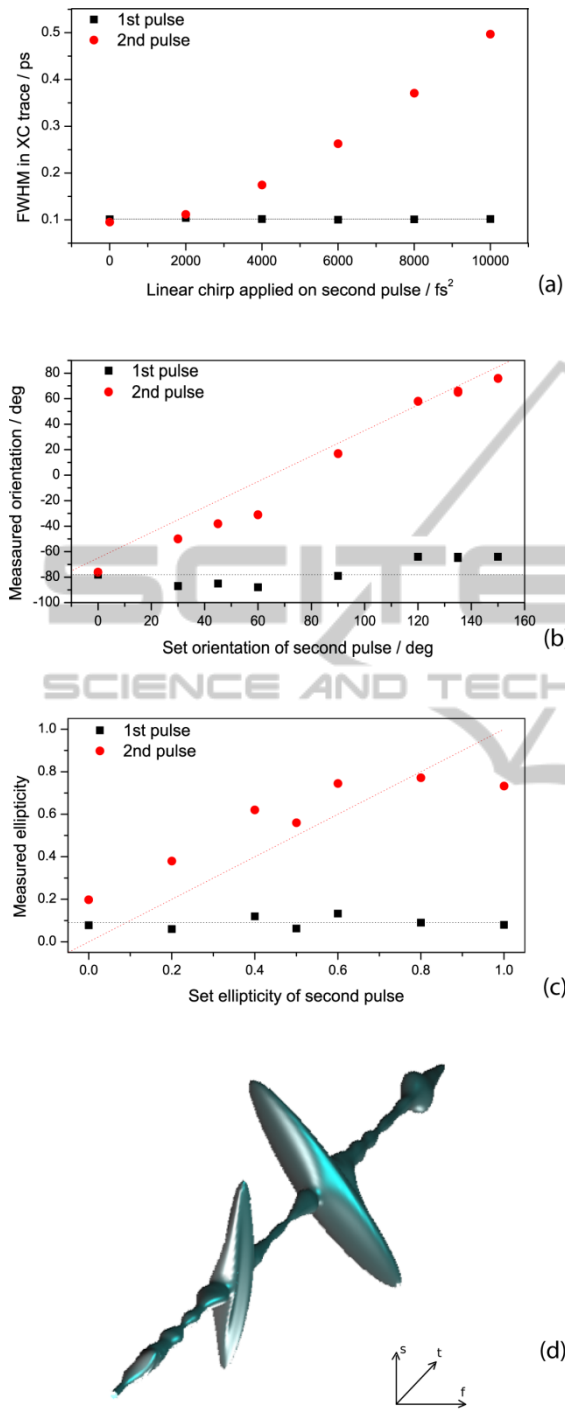


Figure 2: Measured parametric pulse shapes after the hollow core fiber where the linear chirp (a), the orientation (b), and the ellipticity (c) of the second sub-pulse are varied. An exemplary 3-dimensional representation of an experimentally recorded double pulse is depicted in (d) where s and f denote the slow and fast axes, respectively.

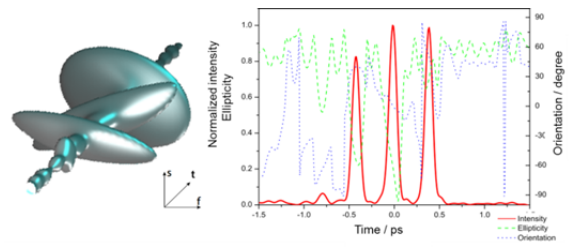


Figure 3: Shape of a complex laser pulse after the fiber. The left side displays a 3-dimensional representation of the measured laser pulse and the right side shows the time-dependent intensity, ellipticity, and orientation.

4 PULSE SHAPING FOR TWO-PHOTON PROCESSES IN DYES

In two-photon processes the photon interference can be utilized by tailored laser pulses to achieve a spectrally narrow two-photon excitation (Meshulach and Silberberg, 1998). This enables selective excitation of different dyes with partially overlapping excitation spectra, which can be applied to two-photon fluorescence microscopy (Ogilvie et al., 2006). The effective two-photon field is due to interference of different components within the laser spectrum $E(\omega)$ and has the form

$$E^{(2)}(2\omega_0) = \int_{-\infty}^{\infty} |E(\omega_0 - \Omega)| |E(\omega_0 + \Omega)| e^{i(\Phi(\omega_0 - \Omega) + \Phi(\omega_0 + \Omega))} d\Omega$$

with the phase function $\Phi(\omega)$ and the center frequency ω_0 . If the phase function is antisymmetric around ω_0 , the exponent vanishes and leaves for $E^{(2)}(2\omega_0)$ the same result as a transform limited pulse with a flat spectral phase (Meshulach and Silberberg, 1998).

In the present contribution sinus phase and third order phase are employed as antisymmetric phase functions. They exhibit constructive interference at the center frequency and partially destructive interference at other frequencies (see Figure 4). With the two photon spectrum and the two-photon cross sections of the involved dyes it is possible to simulate the excitation frequency dependent relative fluorescence intensity I of each dye. This permits to calculate the frequency dependent contrast $(I_{rhB} - I_{cou1}) / (I_{rhB} + I_{cou1})$ between the examined dyes rhodamine B (rhB) and coumarin 1 (cou1).

For the experiment it is very important to precisely control the spectral phase after the fiber by adjusting the pulse shaper settings and carefully

detecting the pulse shape since the measurements are phase sensitive. The measurements were performed

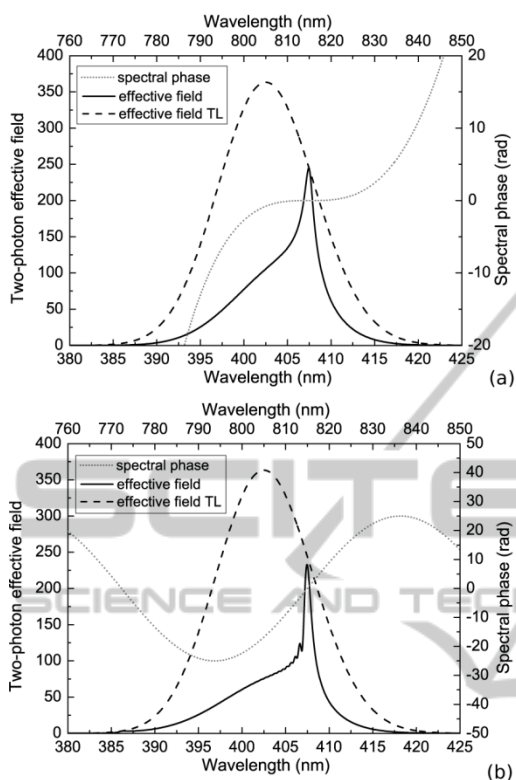


Figure 4: Simulated two-photon field for two antisymmetric phase functions around 815 nm. (a) shows a third order phase function and (b) a sinus phase function. Both two-photon spectra exhibit a sharp peak at the point of antisymmetry at 815 nm which allows selective excitation.

with amplified laser pulses since the non-linear excitation requires substantial pulse energy. The obtained well separated fluorescence spectra of the two dyes enable to record the specific excitation efficiencies by integrating the spectral intensity from 410 nm to 550 nm for coumarin 1 and from 560 nm to 700 nm for rhodamine B.

In Figure 5 frequency scans of the antisymmetric center of the phase functions were performed after the fiber for the sinus and third order phases. The obtained contrast is plotted and shows a good agreement with the simulation results. Higher integrated rhodamine B fluorescence compared to coumarin 1 leads to a contrast larger than zero. For comparison, the contrast obtained for a transform-limited pulse is depicted as a horizontal grey line. The maximal contrast difference is about 0.4 in both cases which allows a clear separation of the dyes. The maximal contrast can slightly be increased by

adding higher Taylor terms to the phase functions since this improves the condition of having

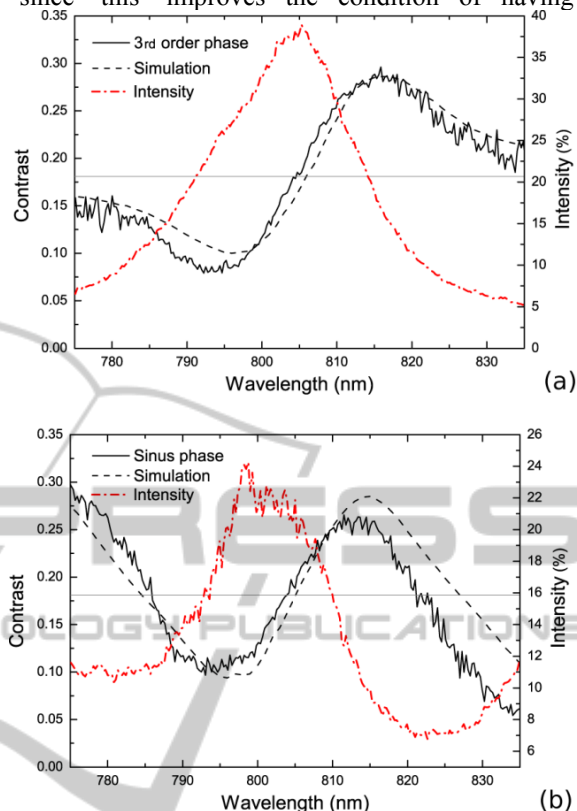


Figure 5: Frequency scans of the point of phase antisymmetry recording the contrast of the two-photon excited fluorescence of rhodamine B and coumarin 1. The intensity is displayed in percentage of a short pulse. A third order phase of $2 \cdot 10^5 \text{ fs}^3$ is used in (a) and a sinus function with an amplitude of 25 rad and a wavenumber of 0.0736 nm^{-1} is applied in (b). The experimental data are in good agreement with the simulations.

constructive interference on one side of the spectrum and destructive interference on the other side. These phase scans on these typical dye markers demonstrate the perspective of pulse shaping after optical fibers for spectroscopic multi-photon applications.

5 CONCLUSIONS

Applications of shaped laser pulses via optical fibers were presented for two-photon processes in dye molecules. The explained phase, amplitude, and polarization forming method employs pre-compensation of the optical fiber properties by analytical pulse shaping to obtain tailored parametric pulse forms at the distal fiber end. In a parametric

sub pulse encoding, the physically intuitive sub pulse parameters including the polarization state were individually controlled.

Moreover, anti-symmetrically phase-shaped pulses after the fiber were applied for two-photon fluorescence of dyes in liquids to enhance the contrast between different dyes with similar excitation spectra. The received experimental results were found to be in good agreement with the conducted theoretical simulations which demonstrates the precision and reliability of the presented method. This novel technique will have perspectives in endoscopic imaging applications by yielding an increased fluorescence contrast.

REFERENCES

- Agrawal, G. P. (2001) *Nonlinear Fiber Optics*, San Diego: Academic.
- Brixner, T., Gerber, G., (2003) *ChemPhysChem*, 4, 418-438.
- Brixner, T., Gerber, G., (2001) *Opt. Lett.*, 26, 557-559.
- Herek, J. L., Wohlleben, W., Cogdell, R. J., Zeidler, D., Motzkus, M., (2002) *Nature*, 417, 533-537.
- Judson, R. S., Rabitz, H. (1992) *Phys. Rev. Lett.* 68, 1500-1503.
- Lozovoy, V. V., Pastirk, I, Walowicz, K. A., Dantus, M. (2002) *J. Chem. Phys.*, 118, 3187-3196.
- König, K., (2000) *J. Microsc.*, 200, 83-87.
- Meshulach, D., Silberberg, Y. (1998) *Nature*, 396, 239-242.
- Myaing, M. T., MacDonald, D. J., Li, X., (2006) *Opt. Lett.*, 31, 1076-1080.
- Ogilvie, J. P., Debarre, D., Solinas, X., Martin, J., Beaulieu, E., Joffre, M. (2006) *Opt. Express*, 14, 759-766.
- Pawłowska, M., Patas, A., Achazi, G., Lindinger, A. (2012) *Opt. Express*, 20, 2709-2711.
- Plewicki, M., Weise, F., Weber, S. M., Lindinger, A., (2006) *Appl. Opt.* 45, 8354-8359.
- Polachek, L., Oron, D., Silberberg, Y., (2006), *Opt. Lett.* 31, 631-633.
- Russel, P (2003) *Science*, 299, 358-362.
- Schäfer-Bung, B., Mitrić, R., Bonačić-Koutecký, V., Bartelt, A., Lupulescu, C., Lindinger, A., Vajda, Š., Weber, S. M., Wöste, L. (2004) *J. Phys. Chem. A*, 108, 4175-4179.
- Tsang, M., Psaltis, D., Omenetto, F. G. (2003) *Opt. Lett.* 28, 1873-1875.
- Tsen, K. T., Tsen, S. W. D., Chang, C. L., Hung, C. F., Wu, T. C., Kiang, J. G. (2007) *J. Phys. Condens. Matter*, 19, 322102-322108.
- Weber, S. M., Lindinger, A., Vetter, F., Plewicki, M., Merli, A., Wöste, L. (2005) *Eur. Phys. J D*, 33, 39-42.
- Weise, F., Achazi, G., Lindinger, A. (2010) *Phys. Rev. A*, 82, 053827.
- Weise, F., Lindinger, A. (2010) *Appl. Phys. B*, 101, 79-91.